Performance Assessment of High-temperature Heat Pump in an Integrated Energy System

Ganesan P

Signe Truyen Ryssdal

Trygve M. Eikevik

Ruzhu Wang

Bin Hu

Performance assessment of high-temperature heat pump in an integrated energy system

P. Ganesan*[1], Signe Truyen Ryssdal[1,2], Trygve M. Eikevik[1], Ruzhu Wang[2], Bin Hu[2],

[1] Department of Energy and Process Engineering, Norwegian University of   Science and Technology, Trondheim, Norway.
Contact Information (pganesanmech@gmail.com, signetr@stud.ntnu.no, trygve.m.eikevik@ntnu.no)

[2] Institute of Refrigeration and Cryogenics, Shanghai, Jiao Tong University, Shanghai, China

*Corresponding author

ABSTRACT

High-temperature heat pumps (HTHP) are known for space and industrial process heating applications. Research on the development of HTHP using natural refrigerant is at a very early stage. In the present work, an HTHP was modeled using MATLAB as part of an integrated energy system. The zero ODP and GWP ammonia (R717) was used as the refrigerant. The main objective of this work is to investigate and optimize the performance and stable operation of the heat pump in an integrated energy system consisting of a PVT system, a battery, thermal energy storage, and a district heating system and to develop the green HTHP. A vapor compression heat pump system with two parallel compressors was used for simulation. The operation of the system was simulated for one year in three Chinese cities: Shanghai, Lanzhou, and Beijing. The heat pump and thermal storage had a maximum capacity of 255.7 kW and 1000 kWh, respectively. The results from the simulations showed that the Heat pump (HP) was able to provide a good temperature lift of 72°C with a condensation temperature of 96°C. The Coefficient of performance (COP) of the HP was 3.55. The system behaved similarly in the three cities during the summer months when temperatures were high and there was little or no demand for space heating. In the colder months, the heat demand in Lanzhou and Beijing was higher than in Shanghai. The gap between available heat and demand was large in Lanzhou and Beijing. It was found that further optimization of the PV panel area, battery, and thermal energy storage is needed to provide a more stable supply of heat and electric power to the HP system.

1. INTRODUCTION

Since the late 1800s, Earth's average surface temperature has risen about 0.9°C, and most of the warming has taken place during the past 35 years (NASA, 2020). According to the Global Status Report from the International Energy Agency in 2017, buildings and construction account for 36% of global energy use and 39% of energy-related CO2 emissions (World Green Building Council, 2017). Operational emissions, that is emissions from heating, cooling, and lighting of buildings, account for 28% of global emissions (World Green Building Council, 2019). As the world is becoming more developed, the demand for heating and cooling will likely rise, as more people will be financially able to equip their residences with heating and cooling systems.

According to the IEA, heat accounted for 50% of final global energy consumption in 2018, and 40% of global CO2 emissions. Around 46% of the heat produced was used in buildings, mainly for space and water heating; 50% was used in industrial processes, and the last 4% was used in agriculture. of all the heat produced in 2018, only 10% came from renewable energy sources (IEA, 2019). Increasing this share by replacing old heating systems with greener, more efficient technologies can contribute greatly to a decrease in global greenhouse gas emissions. Many alternatives exist today, such as district heating systems, solar heaters, and heat pumps. In this work, HTHP is focused on space heating applications. HTHP can produce a condensing temperature of greater than 80°C (Di Wu et al. 2020).

Another way to reduce energy production and consumption emissions is to install an integrated energy system, where various smaller energy systems are connected, communicate, and operate interdependently. Typically integrated energy systems consist of combined cooling, heating, and power (CCHP), but other combinations also exist. Two of the main benefits of integrated energy systems are the reduced overall cost if the system is properly

controlled and the reduced environmental impact due to the higher overall efficiency. Renewable energy sources can be integrated into these energy systems to further reduce the environmental impact.

This paper is part of the project «Key technologies and demonstration of combined cooling, heating, and power generation for low-carbon neighborhoods/buildings with clean energy – ChiNoZEN». The development of green HTHP using an integrated energy system is at an incredibly early stage and that is the focus of this work. The operation of an HP with an integrated energy system is simulated for one year in three Chinese cities Shanghai, Lanzhou, and Beijing. A vapor compression heat pump system with two parallel compressors was used for simulation using MATLAB. The focus of the simulations is to identify the operation and performance of the heat pump using R717, and the goal is to investigate how the heat pump operates with the other components of the integrated renewable energy system.

2. METHODOLOGY

2.1 About the model

The model was created in MATLAB (The MathWorks, 2019), and refrigerant properties were collected from REFPROP (Lemmon et al., 2018). Meteonorm (Meteonorm, 2019) was used to collect weather data from Shanghai, Lanzhou, and Beijing. The electricity demand of other parts of the system than the heat pump was neglected, including the electricity demand for residential use of electrical appliances and lighting. The heat demand for every hour was calculated based on the outside air temperature. A base demand of 50 kW for water heating was assumed to be constant. Additionally, the heat demand increased with decreasing outside air temperatures. The complete system consists of four main components as presented in Fig.1: A PVT system, electrical energy storage, the HTHP, and thermal energy storage. Additionally, the integrated energy system is connected to district heating. Ammonia is a toxic refrigerant at high concentrations and hence needs great care in handling. Sensors are to be installed to detect the leakage. Safety systems like top roof ventilation and ammonia absorption water plant could be the solution to this problem. It cannot be used with copper pipes. otherwise, it is more efficient and costs less than CFC refrigerants.
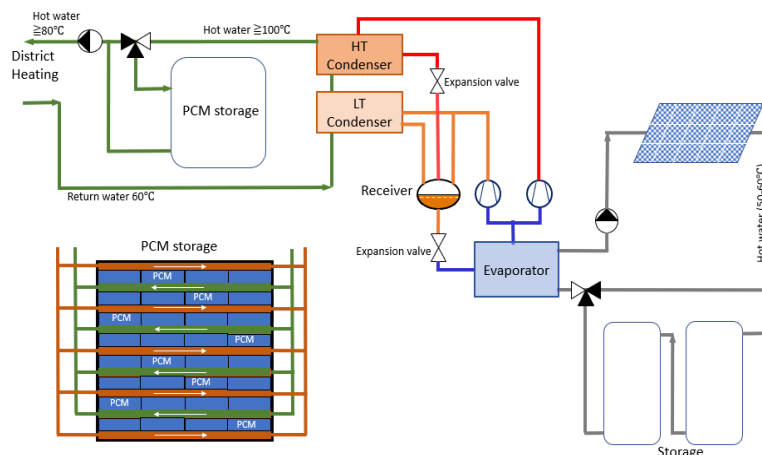
Figure 1: System sketch of the integrated energy system

2.2 Assumptions

The following assumptions were made for the development of the model.

- Any power consumption other than the compressor is neglected.
- Refrigerant at the evaporator outlet is dry saturated.
- Refrigerant at the condenser outlet is wet saturated.
- evaporation and condensation processes are isobaric and isothermal.
- Expansion was isenthalpic, and losses were neglected.

● The inlet temperatures of the water entering the heat exchangers were constant.

2.3 PVT model

The PVT system was simplified in this model. The effects of the solar thermal system were neglected, and only the PV system was modeled. The model of the PV panel and values used in calculations were taken from the datasheet (Jinko Solar, 2020). The total PV area was assumed to be 4000 m², and the performance ratio was assumed to be 75%.

The model of the PV panels consisted of simple calculations that determined the energy output every hour. The modules were assumed to be horizontal, and the hourly values for global horizontal radiation were assumed to accurately represent the radiation the PV system would be exposed to every hour. Any shading effects were neglected. To calculate the energy output, the operating efficiency was first calculated:

$$r = \eta_{STC} - (T_{STC} - T_{PV}) \times T_C \tag{1}$$

Where r is the operating efficiency [%]; η_{STC} is the module efficiency at standard testing Conditions [%]; T_{STC} is the temperature at standard test conditions [°C]; T_{PV} is the surface temperature of the PV module [°C]; T_C is the temperature coefficient of the maximum power point [%/°C].

The electrical energy output from the PV module per hour can be calculated using the equation below:

$$E = A_{PV} \times r \times H \times P_R \tag{2}$$

Where, E is the electric energy generated by the PV module [kWh]; A_{PV} the is surface area of the module [m²]; r is the operating efficiency [%]; H is the global horizontal radiation per hour [kW/m²]; P_R is the performance ratio [%].

2.4 Battery model

The charging and discharging efficiencies are assumed to be 80%, and the maximum storage capacity is 500 kWh. The code for the battery storage is simplified in this simulation. The power added to or removed from the battery is calculated every hour based on power production by the PV system and the compressor's power consumption. If the compressor's power consumption exceeds the power produced by the batteries, the remaining power demand is taken from the battery. If the power consumption is lower than the power production, the excess power is sent to the battery.

2.5 Thermal energy storage model

The thermal energy storage tank is connected to the heat pump and the district heating system. Phase changing materials are used to maintain a temperature slightly above 80°C in the tank so that the heat supply to the district heating system always stays above 80 °C. The specific heat transfer mechanisms between the phase-changing materials and the water are not evaluated. For each hourly iteration, the heat demand is evaluated. The thermal energy system is either charged by receiving energy from the heat pump or discharged by providing energy to the district heating system. Whether the energy storage is charged or discharged depends on whether or not the heat demand exceeds the amount of heat produced by the heat pump. The charging and discharging efficiencies are 90%, and other heat losses are neglected. The maximum storage capacity is 1000 kWh.

2.6 Heat pump model

The heat pump is a vapor compression cycle with an evaporator, an expansion valve, two condensers at different temperature and pressure levels, and two compressors in series. A system sketch can be found in Figure 2 and a pressure-enthalpy diagram is illustrated in Figure 3. For every hourly iteration, the evaporation and condensation temperatures are calculated as well as power consumption, heating capacity, COP, and other properties. The calculations start with initial guesses of the evaporation and condensation temperatures. The refrigerant properties are calculated, and the heat capacity is calculated using the following equation:

$$\dot{Q}_C = \dot{m}_{R,LT} \cdot (h_4 - h_2) + \dot{m}_{R,HT} \cdot (h_7 - h_6) \tag{3}$$

Where, $\dot{Q}_C$ is the total heating capacity in [kW]; $\dot{m}_{R,LT}$ and $\dot{m}_{R,HT}$ are the mass flow rates of the refrigerant through the low-temperature compressor and the high-temperature compressor, respectively, in [kg/s]; h_4 and h_7 refer to the enthalpies at the outlet of the condensers in [kJ/kg], where stage 4 is the outlet of the low-temperature condenser and

stage 7 is the outlet of the high-temperature condenser; h_2 and h_6 refer to the enthalpies at the inlet of the low-temperature and high-temperature condensers.

The power consumption or work done by the compressors in [kW] is calculated and the heating coefficient of performance is calculated with the following equations:

$$\text{Wok done by the compressor } W = \dot{m}_{R,LT} \cdot (h_2 - h_1) + \dot{m}_{R,HT} \cdot (h_6 - h_1) \tag{4}$$

$$COP = Q_c/W \tag{5}$$

Once these values are determined, new values for condensation and evaporation temperatures are calculated. First, the logarithmic mean temperature difference in the condenser is calculated:

$$LMTD_{Condenser} = Q_c/UA \tag{6}$$

Where U is a coefficient that describes the heat transfer through the walls of the heat exchangers in [kW/m²K]. A is the heatexchanger surface area in [m²].
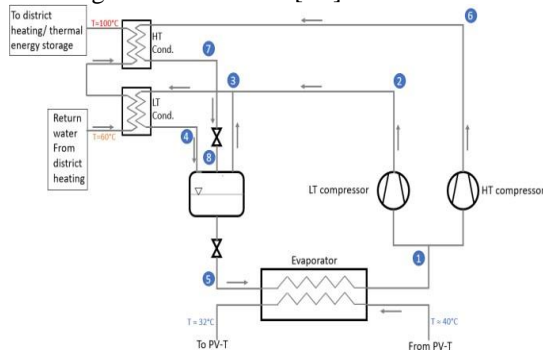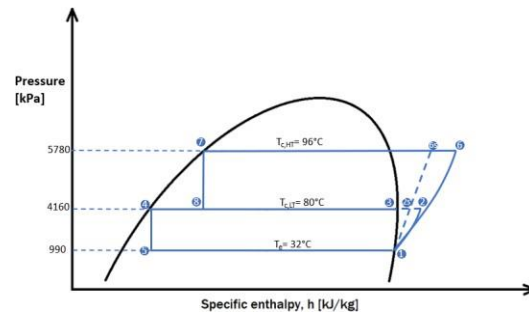

Figure 2: System sketch of the HTHP

Figure 3: Pressure-enthalpy diagram

The outlet temperature of the water heated by the condenser was calculated:

$$T_{hw,out} = T_{hw,in} + \frac{Q_C}{c_{p,hw} \times m_{hw}} \tag{7}$$

$C_{p,hw}$ is the specific heat capacity of the hot waterat constant pressure, in [kJ/kgK]; $\dot{m}_{hw}$ is the mass flow rate of the hot water through the condenser, and $\dot{Q}_C$ is the heat capacity. The unit for all temperatures is °C. Using these values, a new value for the condensation temperature was found using the equation below:

$$T_c = \frac{T_{cw,out} \times e^{\frac{T_{hw,out} - T_{hw,in}}{LMTD_{cond.}}} - T_{cw,in}}{1 - e^{\frac{T_{hw,out} - T_{hw,in}}{LMTD_{cond.}}}} \tag{8}$$

The same is done for the evaporator. If the new value for the condensing temperature deviates from the old value by more than 0.1 °C, the heat pump loop starts again, with the new initial guess for condenser temperature equal to the old value plus half of the difference between the old and the new value. This continues until the difference between the old and new values is less than 0.1°C.

The heat pump is programmed to operate on full load whenever possible. However, when the thermal storage system reaches full capacity, the heat pump is shut off. It remains off until the thermal storage is completely discharged or when the storage capacity is lower than the demand. The heat pump is then turned back on and operates at full capacity until the thermal storage is full. However, if the compressor's power consumption exceeds the available power in the battery and from the PVT system, the heat pump will operate on part load. The load will be as high as possible with the available power supply. The flow chart of the algorithm is presented in figure 4. The load ratio (LR) describes the ratio of the current heating capacity to the maximum capacity (equation 9):
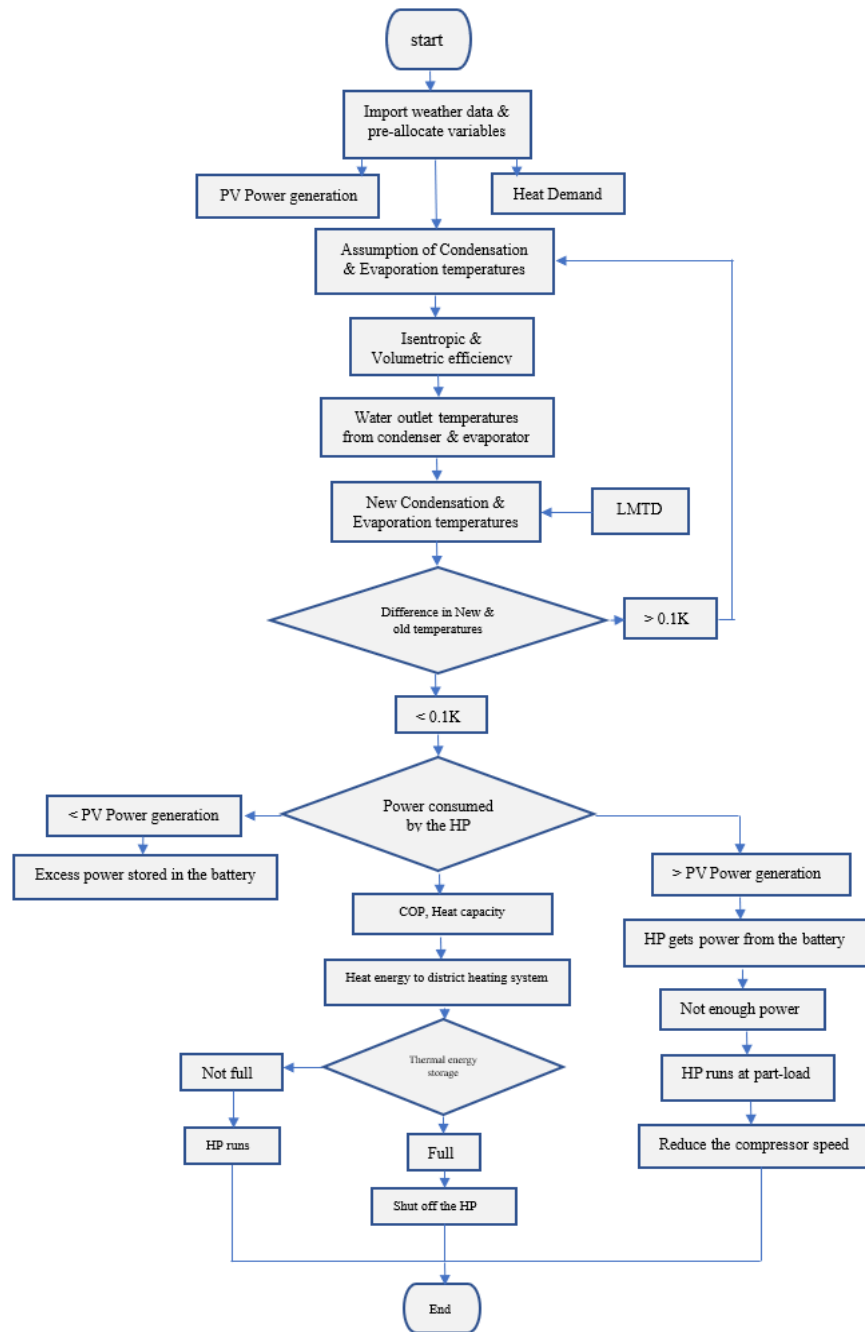
$$LR = \frac{Q_{c,actual}}{Q_{c,max}} \qquad (9)$$

```
                          ┌─────────┐
                          │  start  │
                          └─────────┘
                               │
                 ┌─────────────────────────┐
                 │ Import weather data &    │
                 │ pre-allocate variables   │
                 └─────────────────────────┘
        ┌──────────────────┐        ┌──────────────┐
        │ PV Power         │        │ Heat Demand  │
        │ generation       │        └──────────────┘
        └──────────────────┘
                 ┌──────────────────────────┐
                 │ Assumption of Condensation│
                 │ & Evaporation temperatures│
                 └──────────────────────────┘
                 ┌──────────────────────────┐
                 │ Isentropic &             │
                 │ Volumetric efficiency    │
                 └──────────────────────────┘
                 ┌──────────────────────────┐
                 │ Water outlet temperatures │
                 │ from condenser & evaporator│
                 └──────────────────────────┘
                 ┌──────────────────┐   ┌──────┐
                 │ New Condensation &│◄──│ LMTD │
                 │ Evaporation temps │   └──────┘
                 └──────────────────┘
                 ◇ Difference in New &    ◇──► > 0.1K
                   old temperatures
                 < 0.1K
                 ◇ Power consumed by the HP ◇
```

Figure 4: Algorithm flow chart

3. RESULTS AND DISCUSSION

### 3.1 Heat pump performance and power production

      The system was simulated for the three Chinese cities Shanghai, Lanzhou, and Beijing. Shanghai has the highest annual temperatures and Lanzhou has the lowest temperatures. Due to a greater number of iterations, some results are presented by month or week rather than by year. January is a representative winter month; April is representative of spring and autumn and July is representative of the summer months. Average temperatures, as well

as maximum and minimum values, are displayed in Table 1. Despite large temperature differences during the winter months, the cities have similar temperature and demand curves over a year. Consequently, the same results from all three cities will not be presented. Instead, results from one city will be presented, and the similarities and differences between the three cities will be explained. Figure 5 shows the total heat pump capacity and demand for every hour through the year in Lanzhou.

Table 1: Temperatures [°C] in Shanghai, Lanzhou, and Beijing

	Max. temp.	Min. temp.	Average temp. January	Average temp. April	Average temp. July
SH	38.7	-4.5	4.78	14.56	26.28
LZ	34.5	-16.7	-5.10	11.87	22.61
BJ	38.7	-13.9	-3.92	11.68	27.74

The curves are similar for Shanghai and Beijing, although the hourly demand never exceeds 250 kW in Shanghai. It is clear that the heat demand greatly exceeds the heat pump capacity during certain hours. The heat pump mostly operates at maximum capacity or is shut off. Furthermore, the heat pump operates on part load a few hours throughout the year. The maximum capacity of the heat pump is 255.7 kW.
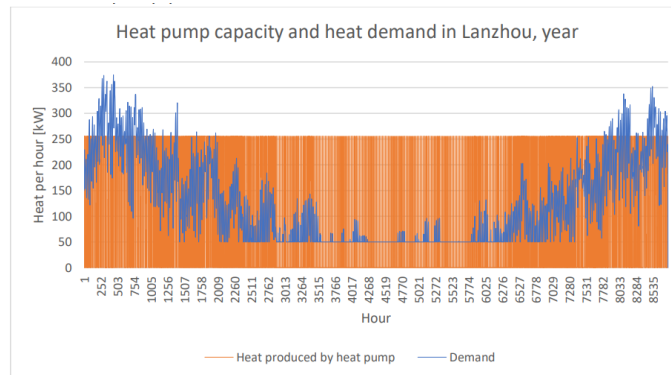
Figure 5: Heat capacity and heat demand in Lanzhou in January

Figure 6 shows the hourly average heat demand and available heat from the heat pump and thermal energy storage per week. The heat supply exceeds the demand most weeks, however, the heat supply is sometimes insufficient during the winter months. Table 2 presents the number of hours with insufficient heat supply. Table 2 is a collection of data that describes heat supply and demand for selected periods. The heat pump operates in less than half the time steps, which means that the heat pump is turned off for more than half the time. In January, the heat pump is turned on for a larger percentage of the time than every year, due to higher demand during the wintermonths. However, the heat pump is turned off more than 40% of the time in all three cities, even though all cities experience heat shortages. The most notable heat shortage is found in Lanzhou, where the heat demand is not met 47.26% of January.

Figure 7 shows the heat production, thermal storage capacity, and heat demand in Lanzhou in January. There is a notable period during the middleof the month when the thermal storage capacity is low or empty, and demand exceeds the amount of heatproduced by the heat pump. It indicates that the heat pump is turned off for several time steps while demand is high. This is because of a lack of available power inthose time steps. To better see the relationship between the lack of heatdespite high demand and a lack of power, figures 8 and 9 will show data for five days in January. There is a clear correlation between the heat pump operation and the available power. The time steps when the heat pump is shut off or is at part load even though demand is high are the same time steps when there is little or no available power for the compressor. This is seen throughout the year and the same results are found in the simulations for Shanghai and Beijing.
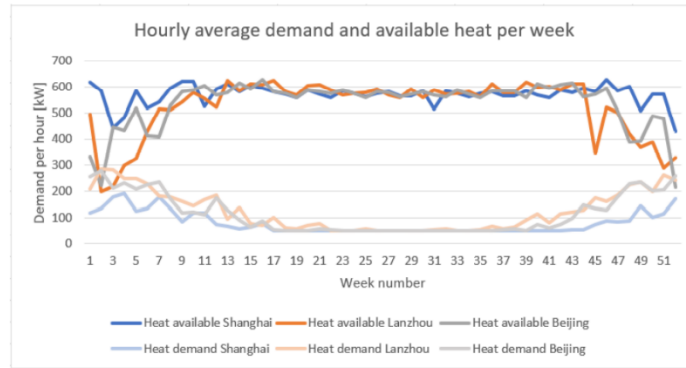
Figure 6: Hourly average heat demand and heat supply

Table 2: Heat shortages

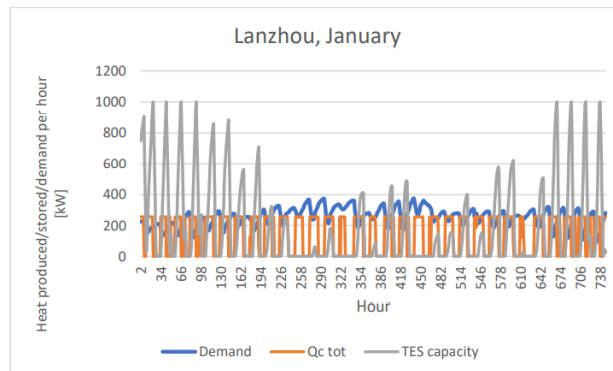|	Number of operating hours heat pump	Percentage e of time when heat pump was turned on [%]	Number of hours when demand exceeds supply	Percentage ge of time with insufficient heat [%]	The total amount of insufficient heat [kWh]
SH Jan.	397	53.14	103	13.79	17 863
LZ Jan.	424	56.76	353	47.26	82 112
BJ Jan.	445	59.57	295	39.49	67 731
SH April	194	26.84	0	0	0
LZ April	285	39.64	9	1.25	874
BJ April	227	31.57	1	0.14	82
SH July	162	21.80	0	0	0
LZ July	162	21.80	0	0	0
BJ July	161	21.67	0	0	0
SH year	2757	31.47	283	3.23	44 795
LZ year	3569	40.75	1090	12.4	236 130
BJ year	3351	38.26	856	9.8	187 534

Figure 7: Heat production, heat demand, and thermal energy storage capacity in Lanzhou in January

To increase the number of operating hours for the heat pump, the amount of available power must be increased. This can be achieved by increasing the area of the PV modules, or by enhancing the battery storage capacity. 9 displays four separate instances where the PV system produces power even when the battery has reached maximum capacity, so increasing the battery capacity would elongate the heat pump operating cycles. Because the battery reaches maximum capacity so many times, increasing the PV area would have little effect without an increase in battery capacity as well. An alternative is to add an auxiliary power supply, for example, wind power, ground-source, or a connection to the local power grid. This would give a more stable power supply, but prices and emissions related to power production would increase.
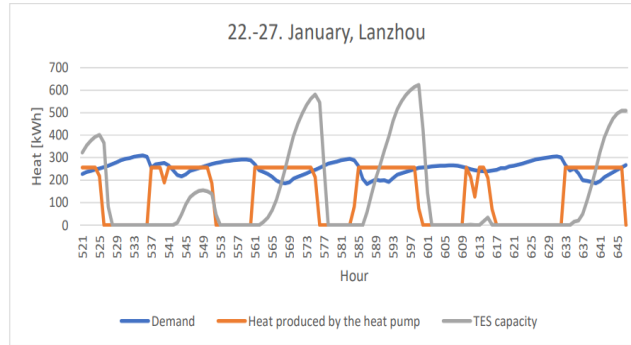
Figure 8: Heat production, heat demand, and thermal energy storage capacity in Lanzhou, January 22-27
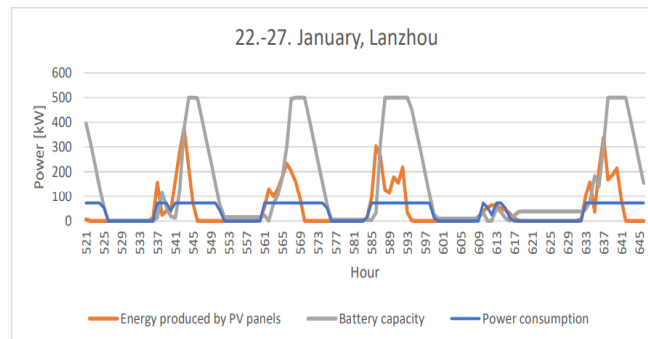
Figure 9: Power production, power consumption, and battery capacity in Lanzhou, January 22-27

Thermal storage capacity or heat pump capacity should also increase if the demand during the winter months is to be met. This must be done together with an increase in available power. The total heat demand in Lanzhou in January was 188 222 kWh. The total amount of heat produced by the heat pump was 105 630 kWh. If the heat pump has been at full capacity for every time step in January, the heat pump would have produced 190 497 kWh. This is slightly more than the total demand, and in theory, it is enough to cover the heat demand in January. However, this assumes a steady heat demand or a higher maximum thermal storage capacity. If the heat demand had been right below 250 kW every hour, the heat pump would always be able to send the heat directly to the district heating system and cover the heat demand. But since the heat demand varies and sometimes approaches 400 kW, the thermal storage unit must supply the heat pump in the hours with the highest demand. To ensure that this can happen, the thermal storage system must have a high enough capacity to save all the excess heat for the heat pump.

Furthermore, the efficiency of thermal energy storage limits the amount of heat that is available. The thermal energy storage system operates with a 90% efficiency during charging and discharging, so 10% of the heat is lost in the process. There are additional heat losses through the walls of the thermal storage system, although those losses have been neglected in this simulation. This means that even if the heat pump operated at full capacity with no breaks every hour throughout January, and even if the thermal storage system had an unlimited capacity, the heat pump in this system would likely not be able to supply the residents in Lanzhou with enough heat to cover their heat demand in January.

Beijing has a slightly lower total heat demand, and it might have been possible to cover this heat demand if an alternative power source was connected to the system and if the thermal storage capacity was higher. The heat shortage in Shanghai in January was 64 249 kWh lower than in Lanzhou, and the heat demand never exceeds 255 kW in any hourly time step. Consequently, the heat pump would be able to cover the total heat demand if an alternative power source were connected so that the heat pump could always operate at full capacity. The heat supply and power demand in July are stable, as can be seen in Figure 10. The results from July and other summer months are remarkably similar for all three cities.

3.2. Temperatures and efficiencies

The condensation temperatures vary greatlythroughout the year. However, it appears that the temperature variations coincide with the load ratio of the heat pump. When the heat pump works on fullload, the heat exchanger temperatures remain relatively constant. While they may vary slightly, they normally stabilize around 80.20°Cin

the low-temperature condenser and 96.02°C in the high-temperature condenser. Thisleads to an outgoing water temperature of 77.82°C from the low-temperature condenser and 92.23°C from the high-temperature condenser. These temperatures are consistent for allthree cities.
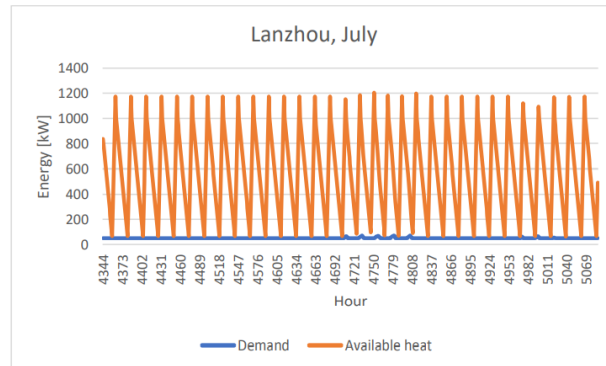
Figure 10: Heat demand and available heat in Lanzhou inJuly

However, at the beginning and end of the year, the temperatures drop quite frequently. Figure 11 displays the temperatures in the two condensers in Shanghai during one week in January. Similar results to the ones displayed in this graph are found throughout the colder periods in all three cities, but the week of January 12 to January 18 was selected to better be able to interpret the results.
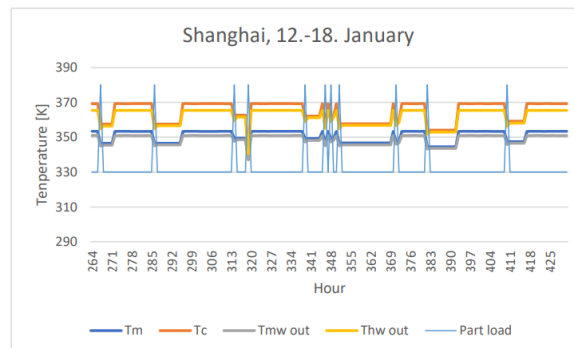

Figure 11: Temperatures in the condensers in Shanghai,January 12-18

As previously mentioned, there appears to be a correlation between the temperature drops and the load ratio of the heat pump. This is also consistent with the literature (Karlsson and Fahlén, 2007). The thin blue, vertical lines showthe time steps when the heat pump operates on part load. An effect on the load ratio is also seen when studying the COP of the heat pump in the various time steps. This is displayed in Figure 12. In Table 3, data from six different time steps are presented. 11-time steps are sorted from largest to smallest load ratio. All the data points are from Lanzhou in January, but similar results are found in the simulation data from the other cities as well. The same results are found during the spring and autumn, but with a lower frequency than in the winter months. There is a clear correlation between the changes in condenser temperatures and COP and the load ratio. The temperatures decrease with the load ratio, while COP increases as the load ratio are reduced.

The outgoing water temperature from the high-temperature condenser normally stays above 80°C, even when the heat pump operates on part load. This is important because the outgoing water temperature to the district heating system is designed to be 80°C. The system will therefore be less efficient and able to transfer less heat to the district heating system if the outgoing water temperature is below 80°C.

A problem occurs when the outgoing water temperature is lower than 80°C, which happens in certain time steps. This happens in less than 5% of the cases, however, this should be avoided to ensure the district heating system receives enough heat. Toavoid this, the heat pump system must be modified so that the condensation temperature of the high-temperature condenser is higher. Because the water temperatures

are related to the load ratio, this problem can also be avoided by limiting the load ratio.
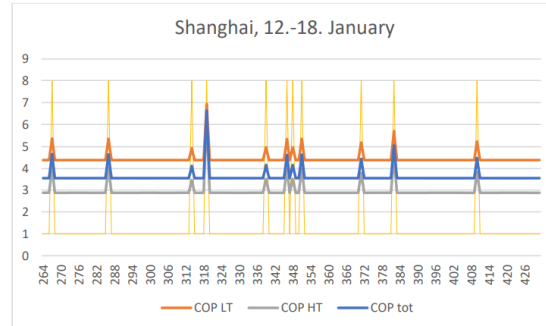
Figure 12: COP of LT cycle, HT cycle, and the total COP for Shanghai, January 12-18

Table 3: Temperature, COP, heat production, and power at different load ratios

Hour	5	378	50	360	7	26
Demand (kW)	228.35	252.95	207.85	264.23	229.38	17.04
Total heat pump capacity (kW)	255.70	218.30	188.44	133.42	67.32	61.01
Load ratio	1.00	0.85	0.74	0.52	0.26	0.24
Total power consumption by the compressors (kW)	72.16	54.76	42.84	25.28	10.46	9.31
Available power (kW)	276.82	57.18	52.65	39.68	17.04	15.67
LT condenser temperature (°C)	80.2	77.13	74.71	70.28	65.09	64.60
HT condenser temperature (°C)	96.02	90.86	86.67	78.96	69.65	68.75
Outlet temp. of water from HT condenser (°C)	92.23	87.56	83.82	76.9	68.55	67.75
COP	3.54	3.99	4.40	5.28	6.44	6.55

The outgoing water temperature drops below 80°C when the load ratio is below 70%. If the heat pump is programmed to shut off when the load ratio drops below 70% ratherthan going on part load, this problem could be avoided, and the outgoing water temperatures would be above 80°C at all times.

Another option is to connect a heating coil to thesystem after the water has passed through both condensers. In this case, there could be a temperature sensor after the high-temperature condenser, and if the temperature is lower than a specified value, for example, 80°C, the heating coil could be turned on. However, this heating coil would require a power source, preferably electricity. The problem is that the heating coil would only be necessary when the heat pump operates on part load, and the heat pump only operates on part load when there is not enough power for the heat pump to operate on full load.

This means that there would not be enough power to heat the heating coil when it was needed. Another drawback is that the heating coil would have a COP below 1 if all losses are accounted for, and the heating coil would therefore reduce the COP of the system.

The increase in COP can be explained by the temperature reduction. Lower condenser temperatures lead to smaller temperature lifts, andless power is needed by the compressor. This results in a higher COP when the condensing temperatures are lower. However, the calculations of COP are not completely accurate due to assumptions and simplifications. The temperature of the heat source is assumed tobe constant. In reality, it is dependent on the ambient temperature and the temperature of the PVT system. The heat source temperature will be higher on hot days and days with a high amount of solar radiation, which leads to the smallest temperature lift and a higher COP. This effect wasneglected in the simulations.

Moreover, the inlet temperature of the water going to the condensers is assumed to be constant. The actual temperature is dependent on the return temperature from the district heating system, which will be affected by mass flow rates and heat demand. Lastly, the power consumption of other components than the compressor is neglected. This includes pumps and other electrical components which need power during heat pump operation. When the heat pump operates on part load, these components make up a larger part of the total power consumption and will lead to a reduced COP (Han et al. 2016). Power consumption also increases during shutdown and start-up, but this effect is neglected.

4. CONCLUSIONS

An HTHP using ammonia refrigerant was simulated using MATLAB. The systems consisted of a PVT system, a battery, thermal energy storage, and a district heating system integrated with HTHP. A vapor compression heat pump system with two parallel compressors was used for simulation. The operation of the system was simulated for one year in three Chinese cities: Shanghai, Lanzhou, and Beijing. The results showed that the HTHP was able to produce a COP of 3.55 with a temperature lift of 72°C with a condensation temperature of 96°C. Similar trends were observed for all cities throughout the year. However, the heat demand was much higher in Lanzhou and Beijing than in Shanghai during the winter months. It was observed that an auxiliary power source must be connected to the system. The capacities of the battery and thermal energy storage must also be enhanced. This will reduce the number of hours with insufficient heat demand and reduce the amount of electrical power produced by the PV system that is wasted due to a full battery capacity.

The heat pump mostly operates on full load, but when there is not enough power, the heat pump operates on part load. This leads to a higher COP due to lower condenser temperatures. However, lower condenser temperatures lead to lower temperatures in the heat sink, which can result in less available heat to the district heating system. The values for COP are not completely accurate due to assumptions about water temperatures and power consumption. However, the individual components are separately modeled and verified that the model is working properly and producing appropriate results and then connected to other system components. There is a need for a more detailed model of the heat pump and the other components in the integrated energy system to get more accurate and realistic values and a better understanding of how the heat pump operates in the integrated energy system. However, the simulations presented in this paper have uncovered certain trends that are important to be aware of in future work. The authors believe that this research will lead international researchers to think about the development of green HTHP as the development of HTHP using natural working fluids is at an exceedingly early stage.

ACKNOWLEDGMENT

REFERENCES

1. NASA. *Climate Change: How Do We Know? (2020)*; https://climate.nasa.gov/evidence/.
2. World Green Building Council. *Global Status Report 2017*. https://www.worldgbc.org/newsmedia/global-status-report-2017.
3. World Green Building Council, (2019) *New report: the building and construction sector can reach net-zero carbon emissions by 2050*, https://www.worldgbc.org/news-media/WorldGBC-embodied-carbon-report-published.
4. IEA. *Renewables 2019*, https://www.iea.org/reports/renewables-2019/heat.
5. Di Wu, Bin Hu, R.Z. Wang, Haibin Fan, Rujin Wang, (2020). The performance comparison of high-temperature heat pump among R718 and other refrigerants. *Renewable Energy 154,* 715-722.
6. Jinko Solar, Tiger Mono-facial 450- 470 Watt. 2020, Jinko Solar.
7. Karlsson, F. and P. Fahlén, Capacity controlled ground source heat pumps in hydronic heating systems, (2007). *International Journal of Refrigeration,* **30** (2): p.221-229.
8. Han, D., Y.S. Chang, and Y. Kim, Performance analysis of air source heat pump system for an office building, (2016). *Journal of Mechanical Science and Technology*, **30** (11): p. 5257-5268.
9. The Math Works, Inc. MATLAB. Version 2019.
10. Lemmon, E.W., Bell, I.H., Huber, M.L., McLinden, M.O. NIST Standard Reference Database 23: *Reference Fluid Thermodynamic and Transport Properties*-REFPROP, Version 9, National Institute of Standards and Technology, Standard Reference Data Program, Gaithersburg, 2018.
11.Meteonorm.com, 2019.